*34th EPS Conference on Plasma Phys. Warsaw, 2 - 6 July 2007 ECA Vol.**31F**, P-5.014 (2007)*

NUMERICAL SIMULATION OF WAKE-FIELD ACCELERATION USING AN EULERIAN VLASOV CODE

M. Shoucri

Institut de recherche d'Hydro-Québec (IREQ), Varennes, Québec, Canada, J3X 1S1

Large amplitude wake fields can be produced by propagating ultrahigh power, short laser beams in plasmas. When the laser power is high enough, the electron oscillation (quiver) velocity becomes relativistic, and large amplitude wake fields are generated. In the laser wake-field accelerator concept, a correctly placed trailing electron bunch can be accelerated by the longitudinal electric field of the wake plasma waves [1]. We study this problem by using an eulerian Vlasov code for the solution of the one-dimensional relativistic Vlasov-Maxwell equations [2]. The code applies a numerical scheme based on a two-dimensional advection technique, of second order accuracy in time-step, where the value of the distribution function is advanced in time by interpolating in two dimensions along the characteristics using a tensor product of cubic *B*-splines [3,4]. We assume the frequency of the laser pulse $\omega_0/\omega_p >> 1$ ($\omega_0/\omega_p = 10$ in the present calculation), and the radiation envelope of the laser pulse changes on a time-scale which is long compared to a plasma period. The spatial length of the laser pulse is $L = \lambda_p = 2\pi c/\omega_p$, much longer than the laser field wavelength λ. The model is similar to what has been presented in [1], with the addition that in the present simulation we include the thermal effects for both electrons and ions by using a kinetic relativistic Vlasov equation, and the evolution of the circularly polarized laser beam is calculated self-consistently with Maxwell's equations.

The pertinent equations

The one-dimensional Vlasov equations for the electron distribution function $f_e(x, p_{xe}, t)$ and the ion distribution function $f_i(x, p_{xi}, t)$ are given by [2,3]:

$$\frac{\partial f_{e,i}}{\partial t} + m_{e,i}\frac{p_{xe,i}}{\gamma_{e,i}}\frac{\partial f_{e,i}}{\partial x} + (\mp E_x - \frac{m_{e,i}}{2\gamma_{e,i}}\frac{\partial a_\perp^2}{\partial x})\cdot\frac{\partial f_{e,i}}{\partial p_{xe,i}} = 0 . \qquad (1)$$

Time t is normalized to ω_{pe}^{-1}, length is normalized to $l_0 = c\omega_{pe}^{-1}$, velocity and momentum are normalized respectively to the velocity of light c, and to $M_e c$. In our normalized units $m_e = 1$ for the electrons, and $m_i = M_e/M_i$ for the ions. The indices e and i refers to electrons and ions. In the direction normal to *x*, the canonical momentum written in our normalized units as $\vec{P}_{\perp e,i} = \vec{p}_{\perp e,i} \mp \vec{a}_{\perp}$ is conserved (the vector potential $\vec{a}_{\perp}$ is normalized to $M_e c / e$). $\vec{P}_{\perp e,i}$ can be chosen initially to be zero, so that $\vec{p}_{\perp e,i} = \pm \vec{a}_{\perp}$. $E_x = -\dfrac{\partial \varphi}{\partial x}$ and $\vec{E}_{\perp} = -\dfrac{\partial \vec{a}_{\perp}}{\partial t}$, $\gamma_{e,i} = \left(1 + \left(m_{e,i} p_{xe,i}\right)^2 + \left(m_{e,i} a_{\perp}\right)^2\right)^{1/2}$. The transverse EM fields E_y, B_z and E_z, B_y for the circularly polarized wave obey Maxwell's equations. With $E^{\pm} = E_y \pm B_z$ and $F^{\pm} = E_z \pm B_y$, we have:

$$(\frac{\partial}{\partial t} \pm \frac{\partial}{\partial x}) E^{\pm} = -J_y \, . \; ; \qquad (\frac{\partial}{\partial t} \mp \frac{\partial}{\partial x}) F^{\pm} = -J_z \tag{2}$$

which are integrated along their vacuum characteristic *x*=*t*. In our normalized units :

$$\vec{J}_{\perp} = \vec{J}_{\perp e} + \vec{J}_{\perp i} \; ; \qquad \vec{J}_{\perp e,i} = -\vec{a}_{\perp} m_{e,i} \int \frac{f_{e,i}}{\gamma_{e,i}} dp_{xe,i} \, . \tag{3}$$

To solve Eq.(1), a 2D interpolation along the characteristics will be used [3,4]. Given $f_{e,i}^{n}$ at mesh points, we calculate the new value $f_{e,i}^{n+1}$ at mesh points from the relations:

$$f_{e,i}^{n+1}(\mathrm{X}_{e,i}) = f_{e,i}^{n}(\mathrm{X}_{e,i} - \mathrm{d}_{e,i}) \; ; \;\; \text{where } \mathrm{d}_{e,i} = \Delta t \mathrm{V}(\mathrm{X}_{e,i} \text{ - } \mathrm{d}_{e,i}/2, t_{n+1/2}) \, . \tag{4}$$

with $\mathrm{X}_{e,i} = \left(x, p_{xe,i}\right)$, and $\mathrm{V}_{e,i} = \left(m_{e,i} \dfrac{p_{xe,i}}{\gamma_{e,i}}, \mp E_x^{n+1/2} - \dfrac{m_{e,i}}{2\gamma_{e,i}} \dfrac{\partial (a_{\perp}^{(n+1/2)})^2}{\partial x} \right)$. The equation for $\mathrm{d}_{e,i}$ in Eq.(4) is solved iteratively, and $f_{e,i}^{n+1}$ is then interpolated using a tensor product of cubic *B*-splines [4]. $\vec{a}_{\perp}^{n+1/2} = (\vec{a}_{\perp}^{n+1} + \vec{a}_{\perp}^{n})/2$ where $\vec{a}_{\perp}^{n+1} = \vec{a}_{\perp}^{n} - \Delta t \vec{E}_{\perp}^{n+1/2}$. To calculate $E_x^{n+1/2}$, a first method calculates E_x^{n} from the solution of Poisson equation, then use a Taylor expansion::

$$E_x^{n+1/2} = E_x^{n} + \frac{\Delta t}{2} \left(\frac{\partial E_x}{\partial t} \right)^n + 0.5 \left(\frac{\Delta t}{2} \right)^2 \left(\frac{\partial^2 E_x}{\partial t^2} \right)^n ; \text{ with } \left(\frac{\partial E_x}{\partial t} \right)^n = -J_x^n ; \; \left(\frac{\partial^2 E_x}{\partial t^2} \right)^n = -\left(\frac{\partial J_x}{\partial t} \right)^n .$$

$$\frac{\partial^2 \varphi}{\partial x^2} = \int f_e(x, p_{x,e}) dp_{x,e} - \int f_i(x, p_{x,i}) dp_{x,i} \, .$$

A second method used in the present work calculates $E_x^{n+1/2}$ from Ampère's equation: $E_x^{n+1/2} = E_x^{n-1/2} - \Delta t J_x^{n}$. Both methods gave the same results.

Results

The EM pulse is excited by propagating in the vacuum at the left boundary the forward propagating circularly polarized laser pulse, written in our normalized units as $E^{+} = 2E_0 \sin(\pi\xi / L)\sin(k_0\xi)$ and $F^{-} = 2E_0 \sin(\pi\xi / L)\cos(k_0\xi)$ for $-L \le \xi \le 0$, $\xi = x - t$, and E_0 =0 otherwise. In vacuum $k_0 = \omega_0 = 10$. The length of the pulse envelope is $L = 2\pi$. We have ten oscillations of the EM wave in the length L of the pulse envelope. We choose for the amplitude of the potential vector $a_0 = 1$, so that $E_0 = \omega_0 a_0 = 10$. Since the envelope is slowly varying, we have for $t < 2\pi$ $a_y = -a_0 \sin(\pi\xi / L)\cos(k_0\xi)$, $a_z =$ $a_0 \sin(\pi\xi / L)\cos(k_0\xi)$. We use a temperature T_e = 3keV and T_i = 1keV. At $t = 2\pi$, the forward propagating pulse has penetrated the domain , and is left to evolve self-consistently using Eqs.(2,3), where $\vec{a}_\perp$ is calculated as indicated in the previous section. Fig.(1) shows the results for the pulse at t= 35.35 (dash curve) which is followed by the wakefield E_x (full curve). The pulse has propagated through the plasma with very little deformation. Fig.(2) shows at t= 35.35 the plot of the electron density (full curve), the ion density (dash curve) and again the axial wake field E_x (dash-dot curve). The amplitude of E_x is growing in space and seems to saturate at 0.6 . This is close to the projected theoretical value for saturation for cold plasma [1] given by $E_{x\max} = (\gamma_0^2 - 1)/\gamma_0 = 0.717$, where $\gamma_0 = \sqrt{1 + a_0^2} = \sqrt{2}$. The electron density (initially equal to 1 in the central region) is forming spikes surrounded by depleted regions, and the electric field E_x is rapidly changing sign at these spikes. Fig.(3) shows the phase-space for the electrons at t=35.35. Particles are accelerated to form a quasi mono-energetic beam (see the 3D view in Fig.(5), which emphasizes the beam spike around $x \approx 20.$). Fig.(4) presents the phase space for the ions, which shows a modulation of the ions distribution function, although the density of the ions shown in Fig.(2) remains essentially identical to the original profile. Figs.(6) and (7) are at t=46.46 when the EM pulse has just left the domain at the right boundary, and are equivalent to Figs.(3) and (2). Note the steeper profile of the electric field in Fig.(7) (dash-dot curve) as we move to the right.

References

[1] P. Sprangle, E. Esarey, A. Ting, Phys. Rev. A 41, 4463 (1990).
[2] S. Guérin, G. Laval, P. Mora, J.-C. Adam *et al.*, Phys. Plasmas 2, 2807 (1995)
[3] M. Shoucri, ‘ The method of characteristics for the numerical solution of hyperbolic differential equations’, in Computer Physics Research Trends (Ed. Silvan J. Bianco, Nova Science Publishers Inc.,NY) (2007); also in Comm.Nonl.Sci.Numer.Simul.(2007)
[4] M. Shoucri, H. Gerhauser, K.-H. Finken Comp. Phys. Comm. 154, 65 (2003).

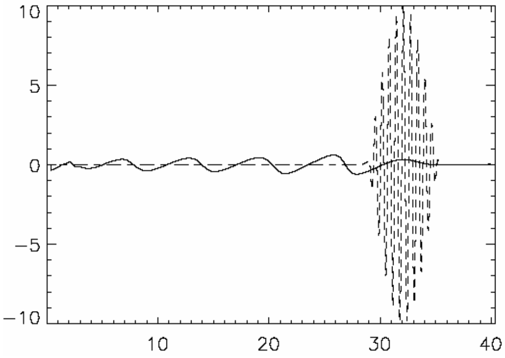

Fig.1

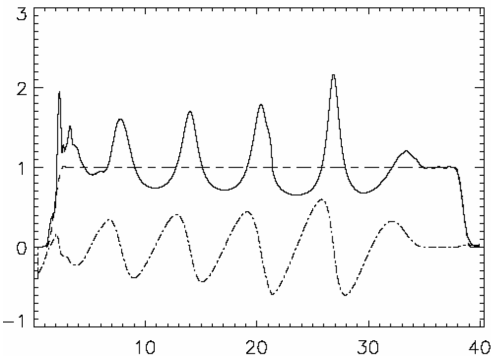

Fig.2

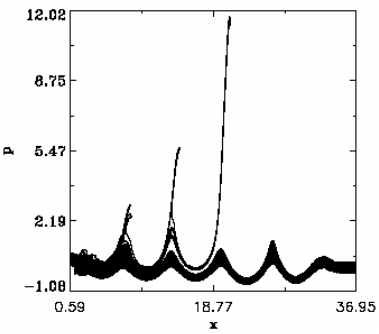

Fig.3

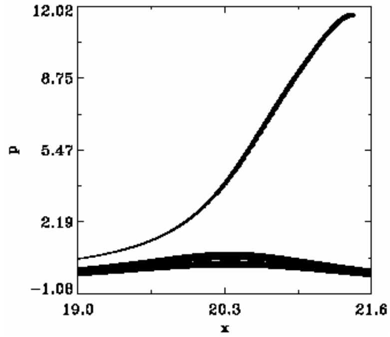

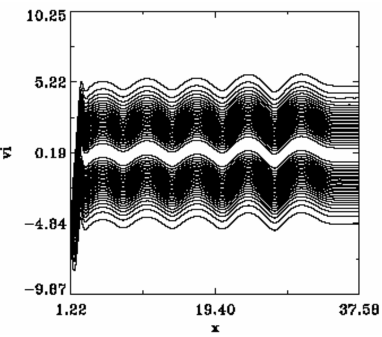

Fig.4

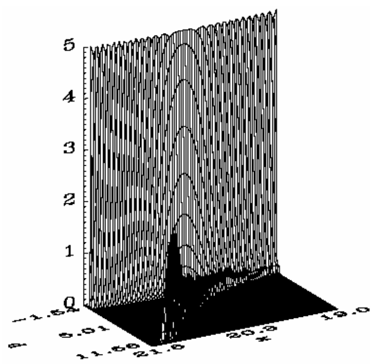

Fig.5

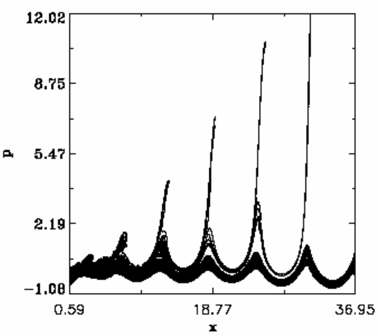

Fig.6

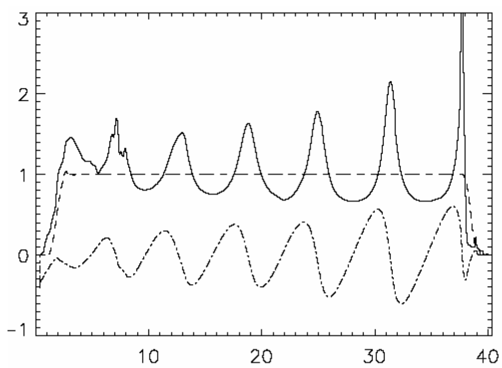

Fig.7